IAEA
International Atomic Energy Agency
Atoms for Peace

23rd IAEA Fusion Energy Conference
11-16 October 2010, Daejon, Korea Rep. of

IAEA-CN-180/ THD/5-1Rb

Comparison between Stellarator and Tokamak Divertor Transport

Y. Feng, M. Kobayashi, T. Lunt, D. Reiter

NIFS-1013

Nov. 01, 2010

Comparison between stellarator and tokamak divertor transport

Y. Feng 1), M. Kobayashi 2), T. Lunt 1), D. Reiter 3)

1) Max-Planck-Institute fuer Plasmaphysik, Germany
2) National Institute for Fusion Science, Toki, Japan
3) Institute for Energy Research-Plasma Physics, Forschungszentrum Jülich, Germany

feng@ipp.mpg.de

Abstract. The paper compares the essential divertor transport features of the poloidal divertor, which is well-developed for tokamaks, and the non-axisymmetric divertors currently investigated on helical devices. It aims at surveying the fundamental similarities and differences in divertor concept and geometry, and their consequences for how the divertor functions. In particular, the importance of various transport terms governing axisymmetric and helical scrape-off-layers (SOLs) is examined, with special attention being paid to energy, momentum and impurity transport. Tokamak and stellarator SOLs are compared by identifying key geometric parameters through which the governing physics can be illustrated by simple models and estimates. More quantitative assessments rely nevertheless on the modeling using EMC3-EIRENE code. Most of the theoretical results are discussed in conjunction with experimental observations.

1. Introduction

Although the divertor idea within the stellarator concept was suggested by Spitzer already in the 50's of the last century [1, 2], intensive exploration of viable divertors for stellarators was started only recently. In contrast, divertor programs in tokamaks began much earlier. After extensive joint research in the tokamak community over several decades, the poloidal divertor as a successful concept has been accepted by most of the existing tokamaks (see e.g. [3,4] and the references therein) and by ITER as well [5, 6, 7]. Divertors for both tokamaks and stellarators follow the same principle, i.e. separating the plasma-surface interaction region topologically from the confinement core by applying appropriate separatrix-bounded magnetic configurations. They aim at similar goals and share the same technology. Divertor transport and physics are subjected to the same atomic and plasma-surface interaction processes and the same fundamental plasma transport processes. In this regard, divertor research recently started on stellarators benefits from the experience and knowledge in both technology and physics gathered in the tokamak community. On the other hand, however, significant differences in divertor geometry and magnetic configuration exist between helical and axisymmetric devices, which influence the plasma, neutral and impurity transport in the SOL and consequently the functionality of a divertor. From this point of view, stellarators open a new window for exploring the optimal divertor solutions for magnetic confinement fusion devices on a broader basis.

Unlike the poloidal divertor in tokamaks, where a separatrix is formed by introducing additional polodial fields, divertor configurations currently explored in helical devices are based on specific edge magnetic structures intrinsically available in each device. Typical examples are the island divertor (ID) for the advanced low-shear stellarators W7-AS and W7-X [8-10], and the local island (LID) and the helical divertor (HD) for the high-shear, largest heliotron-type device LHD [11-14]. An overview of the divertor activities in stellarators is given in [15].

The poloidal divertor preserves the tokamak toroidal symmetry. Smooth flux surfaces can be constructed and ordered in the SOL to provide a natural coordinate-basis for 2D SOL

transport modeling [16-19]. In contrast, the divertor configurations in stellarators exhibit helical structures locally interacting with 3D-shaped divertor plates. Helical SOLs in stellarators are therefore fully 3D and the field lines usually exhibit certain types of stochastic behaviour depending on the field spectrum and the shear at the edge in individual devices. Thus, SOL transport models for helical devices need to meet the increased dimensionality and face the difficulty of dealing with a stochastic field where flux surfaces do not exist. Different concepts and strategies have been explored [20-22]. One example is the EMC3-EIRENE[22, 23] code. It is employed in this paper for physics interpretation of 3D divertor transport and therefore needs a short introduction. EMC3 is a 3D fluid code for both the background plasma and impurities, and solves the fluid equations by applying a Monte-Carlo method on a locally field-aligned vector basis [24]. EIRENE is a 3D kinetic Monte Carlo Code for neutral particles, radiation transfer and kinetic trace ion impurity transport [23]. EMC3-EIRENE was initially developed and applied for W7-AS [22,25-29] and has recently found applications to 3D edge transport problems encountered not only in stellarators [30,31] but also in tokamaks [32-37].

The paper compares the essential divertor transport features of axisymmetric and helical devices. It aims at surveying the fundamental similarities and differences in divertor concept and geometry, and their consequences on the basic function elements of a divertor. Stellarator-specific effects are emphasized while most of the tokamak SOL phenomena are considered to be known with the details being referred to in the literature. Throughout the paper the discussion is guided by simple models and estimates, and the numerical modelling serves to verify their self-consistency. Certain devices and divertor configurations are chosen as examples for the discussion, but the principal conclusions are not restricted to these devices.

2. Large variety of divertor configuration

The geometric principles of the tokamak poloidal-field divertor and of the divertors in helical devices are sketched in figure 1. Low-shear stellarators like the W7-family allow only for the existence of a single island chain at the edge. The rotational transform in the edge region of the LHD HD configurations covers many resonances which overlap and form a stochastic layer of ~10 cm thickness. In the outermost region close to the wall, the increased poloidal field components of the two helical coils create 4 divertor legs which are cut by graphite targets positioned just in front of the wall, forming a divertor configuration similar to the double-null configuration in tokamaks. Nevertheless, the divertor target probes measure rather low downstream densities, typically $< 10^{19}$ m^{-3}, even in high-density operation in LHD [38]. Regarding neutral screening in the present open divertor configuration, the pre-X-point stochastic layer is much “thicker” than the divertor legs and builds the major part of the HD SOL. In this paper, our attention will be paid only to the stochastic layer.

In tokamak SOLs, parallel transport processes clearly dominate and are characterized by the field-line connection length and ion acoustic speed. For describing the divertor transport in stellarators, the situation is more subtle and additional geometric parameters are needed for the following reasons. The contribution of parallel motion to the divertor transport results from a finite field-line pitch Θ. In tokamaks this pitch arises from the external poloidal fields (poloidal divertor), i.e. $\Theta=B_p/B$, and takes a typical value of 0.1. For the island divertor, the divertor-relevant field-line pitch (perpendicular displacement of a field line to targets per

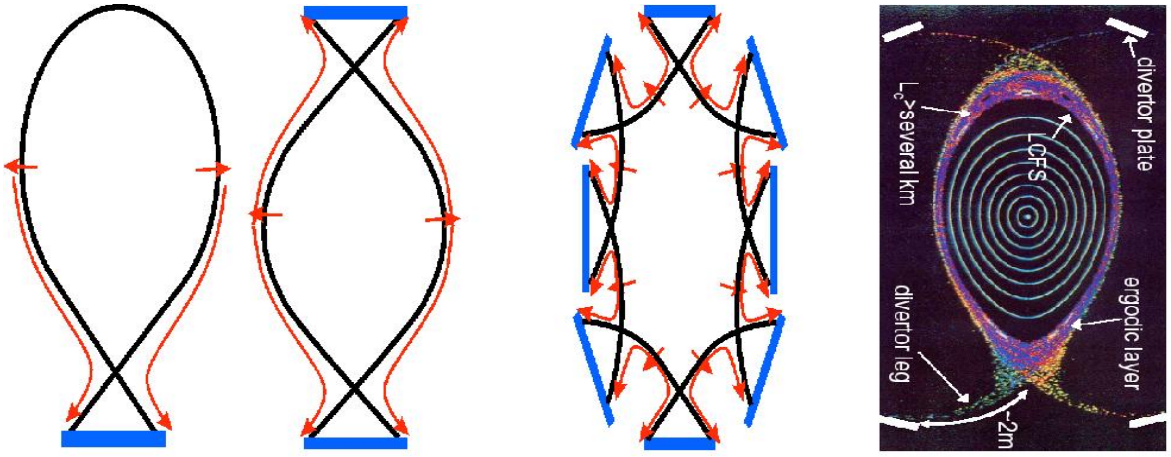

FIG. 1. *Schematics of single-null and double-null tokamak divertors and the intrinsic island divertor for W7-AS and W7-X as well as the helical divertor for LHD. The stochastic layer of the helical divertor in LHD consists of multiple low-order island chains.*

field-line length) arises from a much smaller radial component $B_r(m, n)$ resonant to the n/m rational surface forming the islands, i.e. $\Theta=B_r/B$, typically in the order of 10^{-3}. The open field lines in the stochastic layer exhibit a rather complex evolution structure, yielding a connection length contour ranging from several m to several km. The outermost region is dominated by field lines of short connection lengths. There exist, however, multiple edge surfaces filled by long field lines of several 100 m connection length, forming the main plasma parallel transport channels across the stochastic layer. Thus, the characteristic perpendicular-to-parallel transport scale-length ratio in LHD, i.e. 10 cm SOL thickness divided by several 100 m connection length, is even smaller than those in the IDs of W7-AS and W7-X. For these reasons, the cross-field transport is relatively more important in helical SOLs. In addition, the divertor legs in tokamaks are isolated from each other in terms of cross-field transport (ignoring possible contributions from neutral gas). As a consequence, the plasma pressure (static+dynamic) is constant along the field lines in non-detached divertors. In contrast, in stellarators the SOL often contains regions which are situated close to each other but where the plasma flows in opposite directions. If these regions come close enough to one another, cross-field transport can efficiently transfer momentum from one such channel to another.

3. Extended two-point model for tokamaks and stellarators

The significant differences in divertor geometry in stellarators and tokamaks motivate a rough estimate of the basic physics mechanism involved in the various transport channels. Following the basic idea behind the two-point models for tokamaks [39-41], we develop a 1D model to schematically describe both the stellarator and tokamak SOLs. To this end, we need first to simplify the divertor geometry and reduce the dimensionality of the problem. Here, we introduce the "shortest" perpendicular distance to the target, "x", as our only coordinate. Parallel motion enters the problem through the finite field-line pitch $\Theta=dx/dl_{//}$ with $l_{//}$ being the arc length along the field. Of course, Θ is a function of the two or three coordinates in a realistic SOL, but for simplicity we assume a spatially constant Θ. The 1D transport model then becomes

$$\Theta\frac{d}{dx}\left(-\kappa_{e,i}T_{e,i}^{5/2}\Theta\frac{dT_{e,i}}{dx}\right)+\frac{d}{dx}\left(-\chi_{e,i}n\frac{dT_{e,i}}{dx}\right)=0 \qquad (1)$$

$$\Theta\frac{d}{dx}\left(nV_{\parallel}^2+\frac{p}{m_i}\right)=-\frac{d}{dx}\left(-D\frac{d}{dx}nV_{\parallel}\right)-D\frac{nV_{\parallel}}{\Delta y^2} \qquad (2)$$

$$n_d c_{sd}\gamma T_d = q_{\parallel} \qquad (3)$$

Eq (1) includes the parallel and perpendicular conductive heat transport fluxes for electrons and ions with $n=n_e=n_i$ and $\chi_{e,i}$ being the perpendicular thermal diffusivities. Eq (2) is the parallel momentum balance where $V_{//}$ is the parallel flow velocity and p is the total thermal pressure of ions and electrons. The last two terms in eq (2) represent cross-field momentum transport, which is relevant only for helical SOLs. We first focus on eq (1) and compare the parallel conductive heat flux with the perpendicular one for electrons and ions. For a spatially constant field-line pitch Θ, the ratio of the parallel to the perpendicular heat flux is given by

$$\parallel/\perp=\kappa_{e,i}T_{e,i}^{5/2}\Theta^2/\chi_{e,i}n. \qquad (4)$$

Stellarators differ from tokamaks through the value of Θ. For $\chi_e=\chi_i=2\ m^2/s$, figure 2 shows the $\parallel/\perp$-ratios in the typical SOL parameter range relevant for both stellarators and tokamaks. The four curves represent the $\parallel/\perp=1$ conditions for ions and electrons in a typical tokamak ($\Theta=0.1$) and a stellarator ($\Theta=0.001$), respectively. In most of the SOL parameter domain, $\parallel/\perp>>1$ holds in tokamaks, especially for electrons. Because of the small Θ, the perpendicular and parallel transport are much more comparable in a stellarator SOL, even for electrons. In fact, as shown in figure 2, the *$\parallel$-to-$\perp$* transport ratio in stellarators for both ions and electrons can be tuned from >1 to <1 in experiments either internally by varying the SOL plasma parameters or by externally adjusting Θ. This fine-tuning of the SOL transport has turned out to have a strong impact on impurity transport and the stability of detached plasmas.

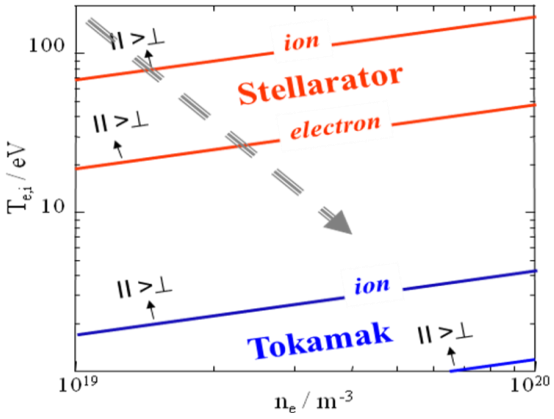

***FIG. 2**. Relative weights of $\parallel$ and $\perp$ conductive heat fluxes of ions and electrons in typical SOL parameter ranges for stellarators ($\Theta=0.001$) and tokamaks ($\Theta=0.1$). The dashed arrow indicates a typical path of SOL plasma with increasing n_e.*

For a qualitative understanding of the role of the momentum loss in divertor transport, we introduce a parameter f_m to represent the integrated effect of the last two terms in eq (2) as

$$p_u = 2p_d(1+f_m) \qquad (5)$$

Replacing the density n in eq. (1) by the averaged upstream and downstream density, $(n_{es}+n_{ed})/2$, we have from eq (1)

$$T_{up}^{7/2}=T_d^{7/2}+\frac{7q_{\parallel}L_c}{2\kappa_e}-\frac{7\chi(n_{es}+n_{ed})}{4\kappa_e\Theta^2}(T_{up}-T_d) \qquad (6)$$

where $\chi=\chi_i+\chi_e$ and κ_i is neglected against κ_e. Eqs (3), (5) and (6) form an extended two-point model for stellarators and reduce to a non-detached tokamak one when $f_m \to 0$ and $\Theta \to \infty$.

We assume $f_m=0$ and $\Theta=0.1$ for (non-detached) tokamaks, and $f_m=\alpha/T_d^{1/2}$ [27] and

$\Theta=0.001$ for stellarators with α being a free parameter representing the strength of the momentum loss. Then, for a given q_{II}, the quantities n_{ed}, T_{up} and T_d can be determined by eqs (3), (5) and (6) using n_{es} as an independent variable. For $q_{II}=0.5MW/(4\pi^2 aR\Theta)$ and $\chi=3m^2/s$, the results are shown in figure 3. The first dashed curve shows the standard two-point model results without cross-field transport as a reference. The sharp change in curve slope at $n_{es}=1\times10^{13}$ cm^{-3} indicates the transition to the high-recycling regime. The solid curves show the results from the extended two-point model including cross-field transport for α=0, 2, 5 and 10. With increasing α the relationship between n_{ed} and n_{es} becomes increasingly linear, and the sharp transition from low to high recycling predicted by the standard two-point model disappears.

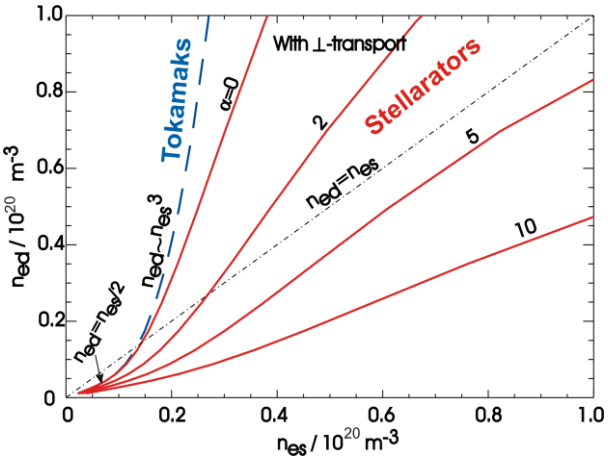

FIG. 3. *n_{ed} vs. n_{es} resulting from the extended two-point model with different strengths of momentum loss compared with standard two-point model for tokamaks.*

Figure 4 compares the EMC3-EIRENE simulation results for W7-AS, W7-X and ASDEX-Upgrade. The same cross-field transport coefficients (D =1 m^2/s and $\chi_{e,i}$=3D) are assumed for the three devices, and the power entering the SOL (P_{SOL}) is linearly scaled with the area of the LCFS, assuming the values of 1, 3, and 10 MW for W7-AS, AUG and W7-X, respectively. The two curves for W7-X correspond to two cases with and without the control coils that can be used to fine-tune the internal pitch of field lines and thereby control the ⊥-to-II transport ratio in the islands. With increasing control-coil current (Icc) and ensuing field-line pitch, the up-/downstream density correlation in W7-X approaches that predicted for the AUG tokamak.

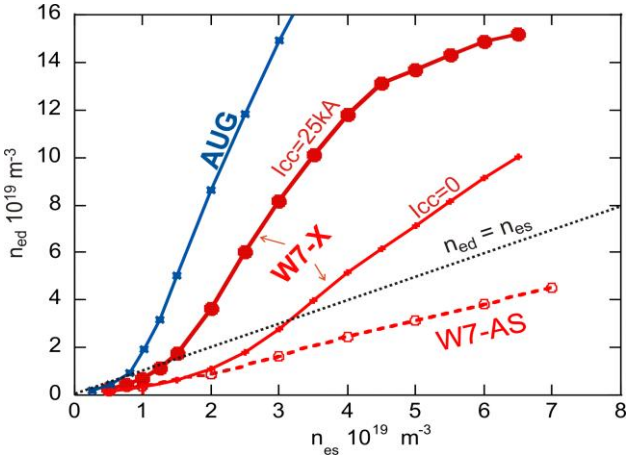

FIG. 4. *Comparison of divertor transport behavior in W7-AS, W7-X and ASDEX-Upgrade calculated by EMC3- EIRENE. n_{ed} is the downstream density whereas n_{es} represents the average density on the LCFS.*

4. Impurity transport

Regarding the impurity and neutral screening, helical SOLs differ from a tokamak SOL in the following respects. (1) In a tokamak SOL, dense and cold plasmas under high recycling conditions are poloidally located in the divertor region. Moving upstream, the SOL plasma becomes “thinner” for CX-neutrals. The wall and other components in the main chamber face an upstream plasma in contact with the core. The helical, multiple-island structure in stellarators spreads out the downstream plasma over almost the entire SOL periphery in both the poloidal and toroidal directions. In other words, a large part of the SOL periphery facing the wall lies “downstream” and protects

the wall from direct exposure to the hot "upstream" plasma. (2) Higher upstream density is needed for helical SOLs to achieve low downstream temperature, because of the geometry-related momentum loss discussed above. Generally, helical divertors can be operated at higher upstream densities than the poloidal divertor in tokamaks, as indeed was shown by both the W7-AS island divertor and the LHD helical divertor. (3) Parallel plasma flows are well distributed in helical SOLs (see figures 9 and 10) and are expected to be able to "flush out" impurities of different origins, including those originating from the wall and targets.

Impurity transport in the complex 3D SOLs of W7-AS, W7-X and LHD has been studied using the EMC3/EIRENE code. The simulation results have shown the existence of a friction-dominated impurity transport regime at high SOL collisionalities for all these devices [27,42-44]. An example is shown for the standard island divertor of W7-X. Using the calculated background plasmas by the Icc=25kA curve in figure 4, test carbon and iron impurities are sampled on the targets (following the deposition distributions of the background ions) and wall (approximated by 20 points quasi-uniformly distributed over one half field period), respectively. Carbon atoms are started mono-energetically with E_0 = 0.1 and 10 eV, which covers the energy range for chemical and physical sputtering processes. Fe-atoms are initiated with E_0=5eV. Figure 5 shows the dependence of the impurity density at the inner separatrix on n_{es} and E_0. The sharp change in the curve-slope at $n_{es} \sim 2\times10^{19}$ m^{-3} indicates the transition from thermal-force to fiction dominated impurity transport in the SOL. A lower n_{es}–boundary is set at 1×10^{19} m^{-3} to exclude the low SOL collisionality cases where the ratio between the connection length and the ion/electron mean free path length is less than 10. As n_{es} is increased to 2×10^{19} m^{-3}, this ratio increases sharply to 100.

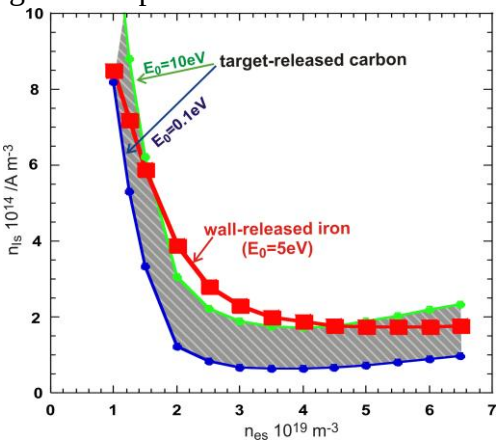

FIG. 5*: SOL impurity retention capability as a function of SOL density predicted for the W7-X island divertor for target-released carbon and wall-released Fe. E_0: initial energy. n_{Is} is impurity density at the inner separartrix normalized to 1A yield for C and Fe.*

5. Summary

The divertor configurations currently explored in stellarators extend the parameter range far beyond that of the "traditional" poloidal divertor in tokamaks. In tokamaks, the nested magnetic flux surfaces are opened by introducing external poloidal fields of comparable strength to that generated by the plasma current. In low-shear stellarators, separatrix-bounded configurations are formed by natural magnetic islands created by much smaller radial perturbation fields inherently existing in the field spectrum of the 3D-shaped coils. The divertor potential of the magnetic islands arises from the internal field-line pitch associated with the shear. The helical divertor configuration in LHD is a natural product of the two helical coils. A pre-X-point stochastic layer of several-cm thickness forms the main part of the SOL which is expected to largely determine the divertor performance of the open HD. In the stochastic layer connection length ranges from m to km. Generally, the divertor-relevant field-line pitch Θ (perpendicular displacement of a field line to targets per field-line length) in stellarators (for the LHD HD at least in the stochastic layer investigated) is much smaller than

in tokamaks.

An extended two-point model is presented, taking both the parallel and cross-field transport into account, where Θ appears as a control parameter for the $\perp$-to-$\parallel$ transport ratio in the SOL. The model addresses the governing transport terms in both tokamaks and stellarators and clearly shows how their relative weights change when Θ varies from the tokamak to the stellarator level. Decreasing Θ beyond the tokamak range to the stellarator level, cross-field heat conduction can dominate over the parallel conduction for the ion energy transport throughout the islands. As the impurity flow velocity driven by the ion thermal force is associated with the classical conductive heat flux, having dominant cross-field heat conduction significantly reduces the thermal-force-driven inward flow of impurities. 3D simulations using the EMC3-EIRENE code based on a trace impurity model have predicted the existence of a friction-dominated impurity transport regime at high SOL collisionalities for all the devices that were investigated, W7-AS, W7-X and LHD. This has also been observed experimentally at high density in W7-AS and LHD.

Helical SOLs are fully three-dimensional and plasma transport is strongly modulated by the helical structure of the island chains. As a consequence, multiple parallel transport channels exist with varying shape and location, resulting in rather complex transport patterns, in particular for the parallel plasma flows. Counter-flows reside on different parts of the helical SOL, and cross-field transport can transfer momentum from one channel to another, causing momentum loss of counter-streaming ions. These geometry-induced effects make the essential transport features of helical SOLs deviate from the standard transport picture realized in tokamaks. For example, the high-recycling regime found in the tokamak poloidal divertor is not observed in W7-AS and LHD, nor is it expected from modelling. From another point of view, stellarators can be operated at higher upstream densities than tokamaks to reach comparably high density, low temperature plasma conditions at downstream.

Another important issue that is not addressed in the paper is the feasibility of thermal power removal via radiation under detachment. In tokamaks, it has been shown that the X-point geometry favours impurity radiation and a strong radiation belt around the X-point, a so-called MARFE [45, 46], is usually observed in detached plasmas. The island chains in helical SOLs provide a multi-null divertor configuration where the number, location and geometry of the X-points can be adjusted externally, thus having the potential of more flexible control of the radiation location for optimum power removal. Indeed, both W7-AS and LHD have demonstrated success in controlling and stabilizing the radiation layer outside the confinement region by externally manipulating the divertor geometry [47, 48]. Numerically it is shown that the plasma-neutral interaction is not the main reason for the rollover of the recycling flux and downstream density in helical devices. The major features of the partially-detached plasma in W7-AS could be well explained by the EMC3-EIRENE code [26]. First simulation results for stable detachment in LHD have also shown similar tendency in carbon radiation pattern as observed experimentally [48]. The code typically shows asymmetric radiation patterns strongly correlated with the geometric details of the low-order magnetic islands. The relevant physics, however, has not been fully understood yet.

References

[1] Spitzer L 1951 *US Atomic Energy Commission Report* NYO-993 (**PM**-S-1)

[2] Spitzer L 1958 *Phys. Fluids* **1** 253

[3] Pitcher C S and Stangeby P C 1997 *Plasma Phys. Control. Fusion* **39** 779

[4] Stangeby P C 2000 *The Plasma Boundary of Magnetic Fusion Devices*, Plasma Phys. Ser., Institute of Physics Publishing
[5] Parker R R 1993 *Plasma Phys. Control. Fusion* B **43** 23
[6] Rebut P H *et al* 1993 *Fus. Eng. Design* **22** 7
[7] Janeschitz G *et al* 1995 *Plasma Phys. Control. Fusion* **37** A19
[8] Kisslinger J *et al* 1995 *Proc. 22nd EPS Conf. on Control. Fusion Plasma Phys.* (Bournemouth, UK) vol **19C** (Geneva: European Physical Society) (part III), p 149
[9] Grigull P *et al* 2001 *Plasma Phys. Control. Fusion* **43** A175
[10] Renner H *et al* 2000 *Nucl. Fusion* **40** 1083
[11] Komori A *et al.*, 2005 *Nucl. Fusion* **45**, 837
[12] Morisaki T *et al.*,2005 *J. Nucl. Mater.* **337-339**, 154
[13] Uo K *et al.*, 1961 *Journal of the physical society of Japan*, vol.**16** 1380
[14] Ohyabu N *et al* 1994 *Nucl. Fusion* **34** 387
[15] König R *et al.* 2002 *Plasma Phys. Control. Fusion* **44** 2365
[16] Braams B 1987 A multi-fluid code for simulation of the edge plasma in tokamaks *NET Report* EUR-FU IXII-80-87-68
[17] Rognlien T D *et al* 1992 *J. Ncul. Mater* **196-198** 347
[18] Simonini R *et al* 1992 *J. Ncul. Mater* **196-198** 369
[19] Schneider R *et al.* 2006 *Contrib. Plasma. Phys.* **46** 3
[20] R. Zagorski et al.,2008 *Nucl. Fusion* **48** 024013
[21] A. Runov et al., 2001 *Phys. Plasmas* **8** 916.
[22] Feng Y *et al* 1999 *J. Ncul. Mater* **266-269** 812
[23] Reiter D *et al* 2005 *Fusion Science and Technology* **47** 172
[24] Feng Y *et al*. 2004 *Contrib. Plasma. Phys.* **44** 57
[25] Feng Y *et al*. 2002 *Plasma Phys. Control. Fusion* **44** 611
[26] Feng Y *et al*. 2005 *Nucl. Fusion* **45** 89
[27] Feng Y *et al* 2006 *Nucl. Fusion* **46** 807
[28] Wagner F *et al* 2005 *Phys. Plasmas* **12** 072509
[29] Hirsch M *et al* 2008 *Plasma Phys. Control. Fusion* **50** 053001
[30] Sharma D *et al* 2005 *Nucl. Fusion* **45** 825
[31] Kobayashi M *et al* 2007 *J. Ncul. Mater* **363-365** 294
[32] Harting D *et al* 2008 *Contrib. Plasma Phys.* **48** (1-3) 1
[33] Frerichs H *et al* 2010 *Computer Phys. Communication* **181** 61
[34] Frerichs H *et al* 2010 *Nucl. Fusion* **50** 034004
[35] Kobayashi M 2007 *Nucl. Fusion* **47** 61
[36] Zha X *et al* 2009 *J. Ncul. Mater* **390-391** 398
[37] Schmitz O *et al* 2008 Nucl. Fusion **48** 024009
[38] Masuzaki M *et al* 2002 Nucl. Fusion **42** 750
[39] Mahdavi A M *et al* 1981 *Phys. Rev. Letters* **47**, 1602
[40] Borras K 1991 *Nucl. Fusion* **31** 1035
[41] Stangeby P C 1993 *Nucl. Fusion* **33** 1695
[42] Kobayashi M. *et al.*, 2009 J. Nucl. Mater. **390–391** 325
[43] Feng Y *et al.*, 2009 *Nucl. Fusion* **49** 095002
[44] Kobayashi M *et al*., 2010 *Fusion Science and Technology* vol. **58** 220
[45] Baker D R *et al* 1982 *Nucl. Fusion* **22** 807
[46] Lipschultz B *et al* 1984 *Nucl. Fusion* **24** 977
[47] Grigull P *et al.*, 2003 *J. Nucl. Mater.* **311–316** 1287
[48] Kobayashi M *et al.*, 2010 *Phys. Plasmas* **17** 056111